Summer 8-19-2021

Analysis of Time-Dependent Adaptations of Lumbar Intervertebral Disc Morphology during Standing-Induced Symptoms of Low Back Pain

Donald Aboytes
Washington University in St. Louis

Washington University in St. Louis

McKelvey School of Engineering

Department of Biomedical Engineering

Analysis of Time-Dependent Adaptations of Lumbar Intervertebral Disc Morphology during Standing-Induced Symptoms of Low Back Pain

By

Donald A. Aboytes

A thesis presented to the McKelvey School of Engineering of Washington University in St. Louis in partial fulfillment of the requirements for the degree of Master of Science

August 2021

St. Louis, Missouri

Acknowledgements

The author wishes to express sincere gratitude to his advisor, Dr. Simon Tang for the immeasurable support and guidance provided throughout this project. He will always be grateful for the opportunity to have learned and developed under the mentorship of such a talented and respected leader in his field. The author also wishes to thank his other thesis committee members Dr. Linda Van Dillen and Dr. Ismael Seáñez. Thank you to all the members of the Tang Lab for their hand in lab-related training as well as their helpful feedback on the project. Special thanks to Dr. Christian Weber for his work which was fundamental to this project. The greatest thanks are owed to his mother Kathryn A. Aboytes, his father Ramón Aboytes-Torres, his sister Carmen N. Aboytes, and his brother Ramón A. Aboytes who have all inspired him to pursue biomedical science and engineering.

Table of Contents

List of Tables iii

List of Figures iv

Abstract v

Chapter 1: Introduction 1

Chapter 2: Methods 4

Participants 4

Data Acquisition 5

Classification of Disc Degeneration 8

IVD Morphometry 8

Disc Height Measurement 9

Missing Observations 11

Statistical Analyses 11

Reliability of Measurements 13

Chapter 3: Results 14

Pain Outcomes 15

Differences in Supine 16

Differences between Supine and Initial Standing 19

Differences during Prolonged Standing 25

VAS Mixed Model 31

Pain AUC and Max VAS Correlations 32

Chapter 4: Discussion 33

Chapter 5: Conclusions 38

References 39

Appendix: Supplemental Materials 44

List of Tables

Table 1 Intra-class correlation coefficients of measurements 13
Table 2 Participant characteristics 14
Table 3 Model results of comparisons in supine 17
Table 3 (continued) 18
Table 4 Model Results of comparisons in supine and standing 20
Table 4 (continued) 21
Table 5 Model results of comparisons in initial standing 23
Table 5 (continued) 24
Table 6 Model results of comparisons during prolonged standing 26
Table 6 (continued) 27
Table 7 Significant correlations with Pain AUC and Max VAS 32

List of Figures

Figure 1. Data acquisition hierarchy diagram 6
Figure 2. Representation of measured parameters 10
Figure 3. Pain progression in PDs 15
Figure 4. Comparisons of female NPDs and PDs 28
Figure 5. Comparisons of male NPDs and PDs 29
Figure 6. Female PDs show different NIDI trajectories from NPDs 30

Abstract

Analysis of Time-Dependent Adaptations of Lumbar Intervertebral Disc Morphology during Standing-Induced Symptoms of Low Back Pain

By

Donald Aboytes

Master of Science in Biomedical Engineering

Washington University in St. Louis, 2021

Research Advisor: Professor Simon Y. Tang

Low back pain (LBP) is a traumatic impairment for individuals with staggering socioeconomic burden. The etiology of LBP is exceedingly complex and confounded by comorbidities. The source of pain is difficult to pin-point because the offending stimuli are not always known. One promising avenue is to investigate the progression of LBP symptoms in young and otherwise healthy individuals. The population that exhibits preclinical LBP in prolonged standing may be particularly suitable for understanding the anatomical changes that occur during the progression of the symptoms. Since the pain symptoms subside upon exiting the standing position, they are an ideal demographic to investigate the initiating pathoanatomical mechanisms of LBP. As the intervertebral discs are thought to give rise to a great proportion of LBP cases, the objective of this thesis is to explore the relationships between standing LBP and the three-dimensional morphology of the lumbar intervertebral discs over time. These relationships were explored in three different stages by comparing those with and without standing LBP in supine, at the time of assuming the standing position, and longitudinally in the standing position for 105 minutes. A 40-participant cohort was recruited and imaged with T2

positional MRI in each stage. Linear mixed models with a time-dependent autoregressive covariance structure were used to evaluate the differences in intervertebral disc morphology between pain developers (PDs) and non-pain developers (NPDs). While the imaging in supine and the initial standing positions alone were not sufficient to detect differences between PDs and NPDs in males or females, inclusion of images over a prolonged standing regimen revealed differences in disc height and the relative signal intensities of the nuclei pulposi in female PDs. There was also a significant correlation between the magnitude of pain and characteristics at certain lumbar levels in both female and male PDs. Future work will focus on identifying specific imaging biomarkers implicated in the initiation of chronic LBP. This study seeks to advance the understanding of the role of the lumbar intervertebral discs in standing LBP to inform future clinical decisions.

Chapter 1: Introduction

Low back pain (LBP) is a musculoskeletal impairment posing a great societal burden affecting up to 80% of people at some point in their life [1–4]. LBP costs the United States up to $200 billion annually due to a combination of direct treatment costs and indirect costs from missed work [5,6]. It is now the leading cause of years lived with disability among the developed and developing world [7,8], and individuals with lower socioeconomic status have disproportionately higher odds of experiencing disabling LBP [9]. Among the most troubling risk factors are work-related stress, depression, and low education [2]. Of note, females experience LBP differently to males having more severe symptoms and greater impairment [10]. There are treatments for LBP [11,12], but in seeking to address its root cause, one encounters the frustrating etiological reality that as many as 95% of LBP cases are non-specific [13] where no pathoanatomical feature can be identified [7].

Even excluding disc herniations, the intervertebral discs (IVDs) are thought to be the cause of up to 42% of chronic LBP cases (a.k.a. discogenic pain) [14]. While no clear pathoanatomical mechanism implicating the IVDs in non-specific LBP has been discovered, intervertebral disc degeneration (IDD) remains among the likeliest candidates. IDD is a chronic condition in which the IVD at one or more segmental levels exhibits structural and biochemical degradation that alters biomechanical function which is thought to initiate LBP. IDD is believed to begin as early as adolescence and becomes more common with age. Despite the incidence of IDD in adult populations both with and without LBP, it is more prevalent in those with LBP than without [15]. Nonetheless, symptomatic and asymptomatic populations both present with overlapping characteristics, and making a diagnosis based on IDD alone is not recommended.

Like the population exhibiting IDD, the population afflicted with LBP is highly heterogeneous[16,17]. In particular, not only are the etiologies complex, but the trajectory and history of the painful condition can vary greatly across individuals. Therefore, approaches to examine populations with a relatively homogeneous LBP history prior to the onset of the chronic disease, may reveal the governing mechanisms for the LBP. There is a preclinical population that experiences inducible LBP symptoms. This population consists of young, back-healthy individuals whose LBP symptoms are induced only by standing for durations close to 2 hours but which are relieved upon exiting the standing position. Pain developers (PDs) are 3 times more likely to experience a near-future bout of clinical LBP than non-pain developers (NPDs) [18]. The involvement of standing in encouraging LBP symptoms is somewhat unsurprising since occupational prolonged standing is consistently identified as a risk factor and potential aggravator of LBP [19–22]. The shared aggravator of LBP symptoms between PDs and some clinical LBP populations only strengthens the interest in this group as the source of the pain may be similar; Furthermore, the toggleable nature of their LBP symptoms and the short time frame in which they develop and subside indicates involvement of the soft tissues in the lower back. These individuals provide us with the ability to explore potential relationships between deformations of the fibrocartilaginous IVDs and LBP symptoms as they arise.

According to previous studies, between 40-60% of young, back-healthy participants develop LBP symptoms [18,23,24]. It has been shown that sensory processing does not differ between these groups [25]. Some postural differences have been observed including greater lumbar lordosis in those that develop pain in the initial standing position [26]. However, the specific predictive features that precede pain development in the lumbar spine remain unknown.

This is an exploratory study investigating the involvement of IVD morphology in pain developed after prolonged standing. Through use of positional Magnetic Resonance Imagining (MRI), we sought to determine whether anatomical differences of the lumbar spine between NPDs and PDs could be resolved before entering the standing positions, after initially entering the standing position, or if any differences would reveal themselves while in the process of developing pain during the prolonged standing task. We hypothesized that differences in IVD morphology, such as those associated with degenerative changes including loss of disc height and reduced NP water content, would require time in a loaded position to develop and that differences in IVD morphology could be level-specific and owing to the greatest potential pain generators. Another objective was to determine the correlative relationship between pain outcomes and the IVD features and whether pain at a given time point could be predicted by any of these features.

Chapter 2: Methods

Participants

The study included back healthy individuals, defined as those with no history of occupational prolonged standing nor any history of LBP, between 18 and 30 years of age with body-mass index (BMI) below 30 kg/m^2. The age of 30 was selected because beyond that age, most people will have experienced LBP [27]. 26 individuals who were part of a prior study [25], and 14 other individuals that met the inclusion criterion, were recruited for this study totaling 40 participants (19 male, 21 female). The participants were recruited from the St. Louis metropolitan area through community announcements and participant registries.

Individuals with any history of clinical LBP were excluded, defined as pain in the lumbar region with a magnitude two or greater on a 0-10 numerical scale; that persisted for 24 hours or more, that subsequently resulted in either: 1) medical intervention from a health care professional; 2) three or more consecutive days of missed work or school; 3) three or more consecutive days of altered activities of daily living. Additional exclusion criterion included any employment history involving standing for longer than 4 hours per day or standing in one place for longer than 1 hour per day in the last year, consumption of greater than 10 alcoholic drinks per week, consumption of greater than 25 caffeinated drinks per week, or smoking more than 15 cigarettes per day, prior diagnosis of anxiety, diabetes, depression, history of trauma to the spine, any surgery on the spine, hip, or pelvis, or lumbar scoliosis, spondylolisthesis, ankylosing spondylitis, herniation of any discs, any pain, numbness, or tingling below the knee, kidney or bladder infection, a history of cancer, or any pain lasting longer than 3 months [28]. Participants were also instructed to avoid non-habitual strenuous physical activity 24 hours prior to imaging.

Data Acquisition

All imaging was performed using a 0.6T Open UPRIGHT® MRI scanner. A 3-plane localizer was adjusted to capture the T2 weighted sagittal image stack of the lumbar spine (repetition time = 610 ms, echo time = 17 ms, field of view = 24 cm, acquisition matrix = 210 × 210, slice thickness = 3 mm, no gap, scan duration = 2 min) [29]. Participants were imaged after spending approximately 15 minutes in the supine position. They were then instructed to stand in the scanner for up to 105 minutes with imaging in 15-minute intervals resulting in 8 standing image stacks per subject. Participants were permitted to exit the scanner at any time, and those that completed at least one scan in both the standing and supine positions were retained in analyses. At each time point, the subject reported the extent of their LBP symptoms on a visual analogue scale (VAS). A VAS rating was made by creating a mark along a 100 mm horizontal line with 0 signifying no pain and 100 signifying the worst pain imaginable. Those with any non-zero LBP for at least two timepoints or arising at their final standing time point were classified as pain-developers (PD), else they were classified as non-pain developers (NPDs). Localization of pain to the lower back was also confirmed using a Body Pain Diagram. Two additional parameters were computed: Max VAS, which is the maximum VAS reported by a subject at any time point and pain AUC, ('Area Under the pain-time Curve') calculated by integrating VAS across time.

Participants laid their wrists on an arm support (VersaRest™) located 5 cm below the lateral epicondyles of the humerus. They were instructed to stand as they normally would and not to lean against the scanner or the arm support. All participants were imaged after 12:00 PM to minimize the effects of diurnal changes to the IVDs [30]. Following acquisition, all images were exported as DICOM files. Data were then anonymized so that the researcher was blinded to

subject identifiers including sex and pain status. Morphometry was performed using 3d Slicer, a free open-source image analysis software, as well as MATLAB (version 2019a) [31–33]. Contrast was set to (W: 800, L:400) and adjusted when necessary to improve visualization of the NP.

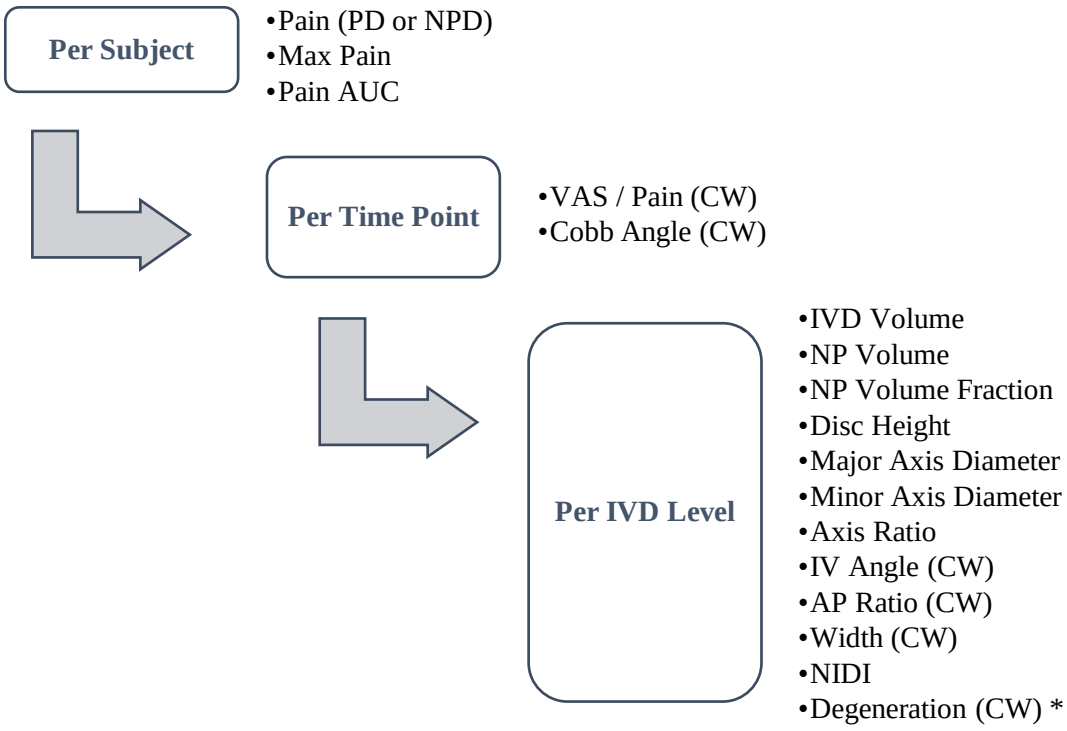

Figure 1. Data acquisition hierarchy diagram. CW denotes measurements performed under another researcher [34]. An asterisk denotes a measurement that was not performed at all time points.

Thirteen parameters were collected from MRI images describing the structure and health of the five lumbar IVDs (L1L2 to L5S1) and the lumbar spine (see Figure 1). Data were collected to describe the geometry and condition of individual IVDs including: a) Whole disc (WD) volume, nucleus pulposus (NP) volume, and NP volume fraction or ratio of the NP volume to WD volume ; b) Major and minor axis diameter (mediolateral and anteroposterior lengths respectively) ; c) Axis ratio, the ratio of major axis diameter to minor axis diameter; d) Central

disc height, hereinafter referred to as disc height, which describes the longitudinal length of the IVD about its centroid; e) Width, which describes disc bulging (despite its similarity to minor axis diameter, it is included in analyses because the method for this measurement is applicable in a clinical setting on single slice MRI images), anterior-to-posterior height ratio (AP ratio) which describes wedging of the discs [34] and intervertebral angle (IV angle) which quantifies the angular contribution of the individual IVD to the whole of the lumbar curvature; e) NIDI, which is the ratio of the mean NP T2 signal intensity to that of the WD and is an indicator of the relative water content of the NP; f) Degeneration, which describes the degenerative status of the disc as assessed by a radiologist. The shape of the lumbar spine was also described with a four-line Cobb angle [34] which quantifies the lordotic curvature of the lumbar spine. Each of these measurements was made in the supine position and at all time points in the standing position except for degeneration which was only measured in the supine position and in the initial standing position.

Classification of Disc Degeneration

Two board-certified radiologists scored, to consensus, the degenerative status of the lumbar IVDs for each participant in the supine position and the initial standing position. The radiologists assessed six aspects of the lumbar IVDs adapted from the Pfirrmann scale: a) Signal intensity of the NP relative to the intensity of other normal discs in the patient; b) Thickness of the annulus fibrosus; c) Disc height and volume relative to other normal discs in the patient; d) Disc bulging or herniation; e) Degenerative changes to the endplates; f) and degeneration of a disc when compared to the other discs in the patient [35]. Each IVD was rated on a scale of 1 to 100, denoting a fully healthy, non-degenerated disc to a highly degenerated disc respectively. Highly degenerated discs correspond to a grade of 5 on the Pfirrmann scale.

IVD Morphometry

First, IVDs and their NPs were contoured inside of sagittal slices [36,37]. Then for each IVD, an oblique viewing plane was adjusted to achieve a mid-transverse cross-section oriented with respect to the IVD of interest. The mid-transverse plane was determined to be the viewing plane which bisects the anterior and posterior boundaries of the IVD across sagittal slices and which bisects the left and right boundaries of the IVD across coronal slices. In this plane, the major and minor axis diameters of the IVD, mediolateral and anteroposterior lengths respectively, were measured [38,39]. The major axis diameter was defined as the length of a line connecting the left and right lateral-most boundaries of the mid-transverse area of the IVD. The minor axis diameter was defined as the length of a mid-sagittal line connecting the anterior-most and posterior-most boundaries of the mid-transverse area of the IVD. Segmentations were stored as binary label maps and passed through a custom MATLAB script where volumes, disc heights, and average signal intensities were calculated.

Disc Height Measurement

This study utilizes a method for measuring disc height directly from IVD voxels identified during segmentation. Whole disc and NP segmentations made in 3dslicer and stored as binary label maps were analyzed using a custom MATLAB script. Voxels of individual WD segmentations were converted to coordinates in 3D space. Principal component analysis was performed on voxel coordinates to obtain a new orthonormal reference coordinate system. This results in three orthogonal vectors of decreasing size which originate from the IVD's centroid. The two largest vectors of the new coordinate system correspond to the directions encompassing the two greatest variances, and when viewing a mid-transverse slice of the IVD, these two vectors tend to point along the mediolateral and anteroposterior axes. The third vector is orthogonal to the mid-transverse plane and therefore represents the longitudinal axis, or z* axis, from which disc height is measured. The first step in our implementation involves isolating voxels on the superior and inferior surfaces of IVD. Surface voxels within a 5mm radius of the z* axis were then isolated to ensure that the height measurement consulted with voxels in at least 3 sagittal slices. Disc height was defined as the difference between the average z* of surface voxels within the ROI above the mid-transverse plane and the average z* of surface voxels within the ROI below the mid-transverse plane. This method offers a consistent, mathematical definition of a disc's longitudinal axis which runs through its geometric center and in which the only observer-influenced variable is the segmentation of the IVD itself.

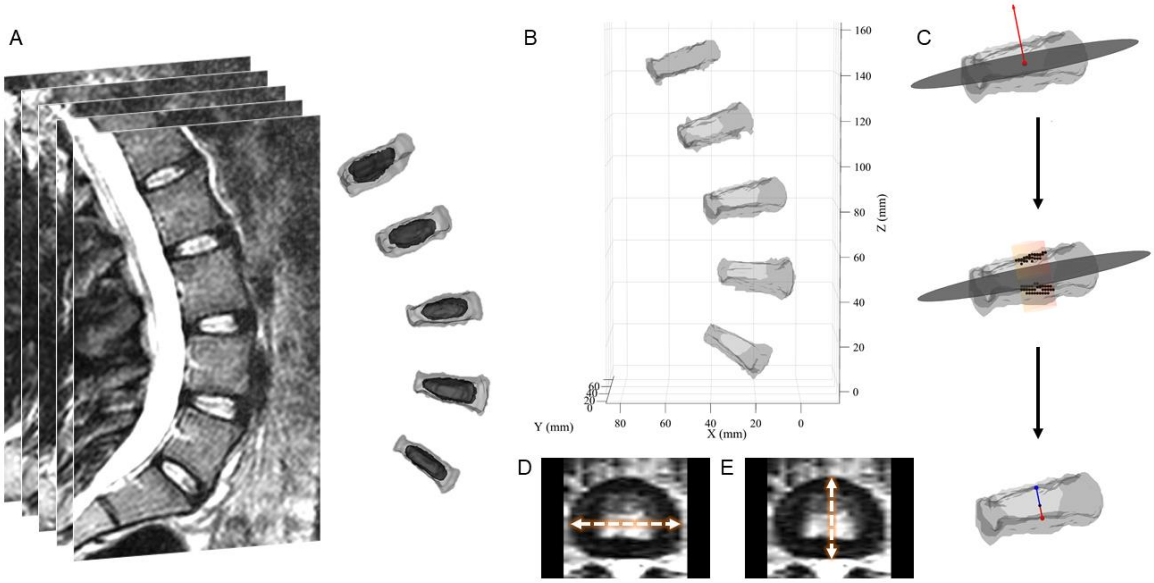

Figure 2. Representation of measured parameters. A) Visual representation of a DICOM stack from which contouring was performed as well as a 3D image of the resulting contoured voxels including the whole IVDs and the NPs of the five segmental levels. B) A mesh representation of a whole IVD segmentation imported to MATLAB including the coordinate system of the localizer region. Note that the z-axis represents the longitudinal axis with respect to the subject. A longitudinal axis with respect to each IVD is described as the z* axis. C) Workflow demonstrating measurement of disc height from identifying the mid-transverse plane (represented by a grey disc) and its z* axis (shown as an arrow), to locating surface voxels surrounding the z* axis, to arriving at the final disc height measurement. D) The major axis diameter which is the mediolateral dimension of the disc. E) The minor axis diameter which is the anteroposterior dimension of the disc.

Missing Observations

In some cases, it was not possible to make robust measurements due to motion artifacts. The imaging procedure calls for the radiologist to establish a localizer scan relative to the subject in his original position. However, because the subject is in an unsupported position while standing, their body can shift throughout the scan resulting in cutoff or imaging artifacts. This resulted in random loss of some observations. In most cases, an observation was omitted for some parameters but not others. For example, an IVD that is partially outside of the scanned region results in loss of a whole disc volume measurement but not minor axis diameter measurement for that disc. Imputation of missing data was only performed for one analysis. Missing observations were replaced by linearly interpolating between the nearest adjacent time points if available.

Statistical Analyses

Analyses for data measured from female and male participants were performed separately to account the sex-specific anatomical variations in the spinal column. With the measured parameters as response variables, linear mixed effects models were used to model main effects of pain, disc level, and time in the standing position as well as their pairwise interactions. BMI was included in the models as a covariate. Random effects were modeled for subjects, and segmental levels were nested within subjects where applicable. When time was included as a fixed factor, repeated measures for the random effects were modeled with an autoregressive covariance structure with adjacent serial weighting of covariances. In analyses in which there was no source of non-independence within the data, such as when Cobb angle was assessed at a single time point, a general linear model was utilized instead of a mixed model.

A separate linear mixed effects model was used to fit a multivariate regression with raw non-zero VAS ratings as the response variable and the aforementioned morphological features of the lumbar IVDs and lumbar spine as explanatory variables. In this case, the morphological parameters of the IVDs were striated by disc level and included as their own explanatory variables. Moreover, BMI was not included as a covariate as the range of BMI is too narrow for theoretical involvement in predicting painful VAS scores. VAS was log-transformed to address non-normally distributed residuals. Model selection was informed by a backward stepwise selection algorithm in which fixed factors were sequentially removed until the model saw no improvement in the Bayesian Information Criterion (BIC) defined as a decrease in BIC greater than 0.5. BIC was selected over the Akaike Information Criterion (AIC) because unlike BIC, AIC is prone to permitting selection of overly complex models as it does not account for the number of observations in the model [40,41].

Linear mixed effects models were performed in R programming language (RStudio) using the nlme package (v3.1-152; Pinheiro et al., 2021). Results are reported for type III tests of fixed effects in the presence of interactions and type II tests in their absence. Significance of all statistical results were determined with alpha at 0.05.

Post hoc multiple comparisons are reported after applying either a Šidák adjustment for planned contrasts or a Tukey's HSD adjustment. Post hoc power was calculated using the nlmeU package in R (v0.70-3; Galecki et al., 2015). Standardized effect sizes are reported as partial eta-squared calculated using the effectsize package in R (v0.4.5; Ben-Shachar et al., 2021).

Reliability of Measurements

The intra-rater reliability of all parameters measured by the researcher (D.A.) was determined via the intra-class correlation coefficient using IBM SPSS Statistics (Version 27) based on a single measures, absolute agreement, two-way mixed effects model. Measurements for 10 randomly selected IVDs were repeated on three non-consecutive days. All ICC estimates demonstrated moderate to excellent repeatability. ICC results can be found in Table 2. Intra-rater and inter-observer ICCs for the other measured parameters were also moderate to excellent [34].

Table 1

Intra-class correlation coefficients of measurements. SI stands for Signal Intensity.

Measurement	ICC [95% CI]
IVD Volume	0.87 [0.55 – 0.97]
NP Volume	0.87 [0.43 – 0.97]
Disc Height	0.95 [0.88 – 0.99]
IVD S.I.	0.99 [0.98 – 0.99]
NP S.I.	0.93 [0.64 – 0.98]
Minor Diam	0.94 [0.81 – 0.99]
Major Diam	0.79 [0.52 – 0.94]

Chapter 3: Results

36 individuals completed all standing time points. Three PDs were not able to complete the study due to excess pain or discomfort. Two of these participants completed all but one time point while the third participant exited after only two standing time points. One NPD was unable to complete the final three time points due to system issues. Half of the participants developed LBP during standing with 12 female PDs to 9 female NPDs and 8 male PDs to 11 male NPDs. Female PDs weighed less than NPDs ($p < 0.05$ using an independent t-test); however, they did not differ in age, height, or BMI. Male PDs did not differ from NPDs in any characteristic.

Table 2

Participant characteristics. Reported p values are results of two-tailed independent t-tests.

	Female			**Male**		
	NPD (9)	**PD (12)**	**p value**	**NPD (11)**	**PD (8)**	**p value**
Age (y)	25.3±1.7	24.6±2.5		24.9±2.8	24.4±4.6	
Height (cm)	167.9.0±7.6	162.2±7.7		179.1±8.3	177.7±6.9	
Weight (kg)	63.5 ± 5.4	57.6±4.2	= 0.012	76.4±9.2	69.1±8.2	= 0.093
BMI (kg/m^2)	22.7±1.8	22.2±2.2		23.8±2.3	21.9±2.4	= 0.092

Pain Outcomes

Around half of the PDs reported their first LBP symptoms by 30 minutes of continuous standing and their maximal LBP symptoms by 90 minutes. Males and females demonstrated similar trends in pain progression.

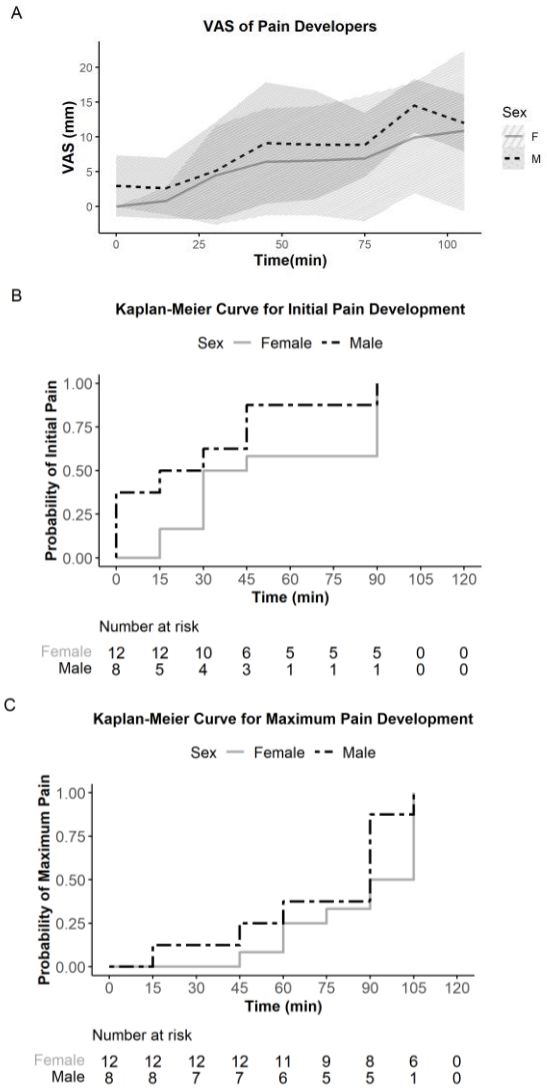

Figure 3. Pain progression in PDs. Results are separated by sex. A) VAS rating across time with lines representing the mean VAS and the shaded regions representing the mean ± the standard deviation. B) Survival curves showing the probability of a PD experiencing the first symptoms of LBP during prolonged standing. C) Survival curves showing the probability of a PD developing their worst LBP symptoms during prolonged standing.

Differences in Supine

The pain status of an individual in supine was not predictive of IVD morphology nor Cobb angle. The linear model for Cobb angle yielded a poor fit on the male data. In males, post hoc comparisons of degeneration between lumbar levels revealed that the L5S1 disc level was more degenerated than all other disc levels ($p < 0.01$ for all comparisons; Tukey) and that no other discs differed from each other in degeneration.

Table 3

Model results of comparisons in supine. For mixed models, R_c^2 is reported which signifies the variance explained by fixed and random effects [42].

	Female				Male			
	Pain Status (PS)	Lumbar Level (LL)	BMI	PS x LL	Pain Status (PS)	Lumbar Level (LL)	BMI	PS x LL
IVD Volume		***				***		
p value		< 0.001				< 0.001		
η_p^2		0.54				0.62		
95% CI		[0.38, 0.65]				[0.45, 0.72]		
1 - β		1				1		
R^2		**R^2_c = 0.76**				**R^2_c = 0.81**		
NP Volume		***				***		
p value		< 0.001				< 0.001		
η_p^2		0.48				0.51		
95% CI		[0.00, 0.18]				[0.33, 0.63]		
1 - β		1				1		
R^2		**R^2_c = 0.75**				**R^2_c = 0.68**		
NP Volume Fraction		**				***		
p value		< 0.001				< 0.001		
η_p^2		0.19				0.34		
95% CI		[0.03, 0.32]				[0.12, 0.48]		
1 - β		0.91				0.99		
R^2_m		**R^2_c = 0.72**				**R^2_c = 0.65**		
Disc Height		***				***		
p value		< 0.001				< 0.001	= 0.06	
η_p^2		0.55				0.63	0.20	
95% CI		[0.38, 0.65]				[0.47, 0.72]	[0.00, 0.51]	
1 - β		1				1	0.47	
R^2		**R^2_c = 0.49**				**R^2_c = 0.65**		
Major Axis Diameter		***				**		
p value		< 0.001				< 0.01		= 0.10
η_p^2		0.35				0.21		0.13
95% CI		[0.16, 0.48]				[0.02, 0.36]		[0.00, 0.26]
1 - β		1				0.9		0.58
R^2		**R^2_c = 0.79**				**R^2_c = 0.66**		
Minor Axis Diameter		***				***		
p value		< 0.001				< 0.001		
η_p^2		0.28				0.27		
95% CI		[0.10, 0.41]				[0.08, 0.41]		
1 - β		0.99				0.97		
R^2		**R^2_c = 0.72**				**R^2_c = 0.83**		

Table 3 (continued)

	Female				Male			
	Pain Status (PS)	Lumbar Level (LL)	BMI	PS x LL	Pain Status (PS)	Lumbar Level (LL)	BMI	PS x LL
Axis Ratio								
p value								
η_p^2								
95% CI								
1 - β								
R^2		**R^2_c = 0.59**				**R^2_c = 0.33**		
IV Angle		***	**			***		
p value		< 0.001	< 0.01			< 0.001		
η_p^2		0.72	0.37			0.72		
95% CI		[0.61, 0.79]	[0.05, 0.62]			[0.60, 0.79]		
1 - β		1	0.87			1		
R^2		**R^2_c = 0.71**				**R^2_c = 0.70**		
AP Ratio		***				***		
p value		< 0.001				< 0.001		
η_p^2		0.58				0.63		
95% CI		[0.43, 0.68]				[0.48, 0.72]		
1 - β		1				1		
R^2		**R^2_c = 0.53**				**R^2_c = 0.60**		
Width		**				***		
p value		< 0.01				< 0.001		
η_p^2		0.19				0.37		
95% CI		[0.03, 0.32]				[0.17, 0.50]		
1 - β		0.92				0.99		
R^2		**R^2_c = 0.73**				**R^2_c = 0.85**		
NIDI		***				***		
p value		< 0.001				< 0.001		
η_p^2		0.28				0.4		
95% CI		[0.09, 0.42]				[0.19, 0.53]		
1 - β		0.99				1		
R^2		**R^2_c = 0.52**				**R^2_c = 0.67**		
Degeneration						***		
p value		= 0.07				< 0.001		
η_p^2		0.12				0.3		
95% CI		[0.00, 0.24]				[0.10, 0.44]		
1 - β		0.63				0.99		
R^2		**R^2_c = 0.17**				**R^2_c = 0.24**		
Cobb Angle								
p value								
η_p^2								
95% CI								
1 - β								
R^2		**R^2 = 0.14**				**R^2 = 0.01**		

Differences between Supine and Initial Standing

Whole disc volume in males and females were reduced after assuming the standing position. The estimated differences in IVD volume between supine and standing was 0.279 cm^3 in females and 0.69 cm^3 in males. Female disc height decreased by 0.151 mm ($p = 0.0269$) after standing but did not significantly change in males. Females saw a small but significant decrease in Cobb angle after entering the standing positions (3.44 degrees, $p = 0.04$). The degeneration of the L5S1 level increased after standing by 1.69 in females ($p < 0.001$; Šidák) and increased by 2.87 in males ($p < 0.001$; Šidák). In males, the L5S1 minor axis diameter alone saw a significant increase of 0.97 mm ($p = 0.0305$; Šidák) after standing. In both females and males, the L5S1 IV angle alone decreased after assuming the standing position with females seeing a decrease of 3.48 degrees ($p < 0.0001$; Šidák) and males seeing a decrease of 2.48 degrees ($p = 0.0010$; Šidák). Likewise, the AP ratio of just the L5S1 IVDs were significantly changed after standing, with the L5S1 AP ratio of females decreasing by 0.43 ($p < 0.0001$; Šidák) and of males decreasing by 0.42 ($p =0.0003$; Šidák). NIDI was different according to disc level in both males and females. In females, the estimated mean NIDIs from the L1L2 to L5S1 levels were 1.58, 1.66, 1.60, 1.48, and 1.44, with L5S1 being significantly lower than L3L4 and L2L3 ($p = 0.0009$, $p = 0.0271$; Tukey) and with L4L5 being significantly lower than L2L3 ($p = 0.0154$; Tukey). In males, the estimated NIDIs from L1L2 to L5S1 were 1.70, 1.84, 1.88, 1.67, and 1.53, with the L5S1 NIDI being lower than L2L3 and L3L4 levels ($p = 0.0001$, $p < 0.0001$; Tukey) and the L4L5 level being lower than L3L4 ($p = 0.0218$; Tukey). There was a significant pain and position interaction on female NIDI showing that female NPDs saw no change in NIDI between supine and standing while the PDs saw a small but significant drop of 0.093 after standing ($p = 0.0002$; Šidák).

Table 4

Model Results of comparisons in supine and standing.

	Female					Male				
	Pain Status (PS)	Lumbar Level (LL)	Position (O)	BMI	Interaction	Pain Status (PS)	Lumbar Level (LL)	Position (O)	BMI	Interaction
IVD Volume		***	*				***	***		
p value		< 0.001	< 0.05				< 0.001	< 0.001		
η_p^2		0.59	0.05				0.64	0.17		
95% CI		[0.43, 0.68]	[0.00, 0.26]				[0.48, 0.73]	[0.04, 0.32]		
1 - β		1	0.65				1	0.94		
R^2			**R^2_c = 0.94**					**R^2_c = 0.94**		
NP Volume		***			**		***			
p value		< 0.001	= 0.07		PS x O < 0.01		< 0.001			
η_p^2		0.55	0.02		0.10		0.52			
95% CI		[0.39, 0.66]	[0.00, 0.10]		[0.02, 0.22]		[0.34, 0.64]			
1 - β		1	0.45		0.90		1			
R^2			**R^2_c = 0.92**					**R^2_c = 0.94**		
NP Volume Fraction		**			**		***	*		
p value		< 0.01			PS x O < 0.01		< 0.001	< 0.05		
η_p^2		0.20			0.07		0.4	0.07		
95% CI		[0.04, 0.33]			[0.01, 0.19]		[0.20. 0.54]	[0.00, 0.21]		
1 - β		0.93			0.78		1	0.59		
R^2			**R^2_c = 0.86**					**R^2_c = 0.86**		
Disc Height		***	*				***			
p value	= 0.054	< 0.001	< 0.05	= 0.062			< 0.001			
η_p^2	0.19	0.60	0.06	0.18			0.63			
95% CI	[0.00, 0.48]	[0.45, 0.70]	[0.00, 0.18]	[0.00, 0.47]			[0.48, 0.72]			
1 - β	0.50	1	0.61	0.48			1			
R^2			**R^2_c = 0.90**					**R^2_c = 0.92**		
Major Axis Diameter		***			**		***			
p value		< 0.001			LL x O < 0.01		< 0.001			
η_p^2		0.37			0.16		0.29			
95% CI		[0.19, 0.50]			[0.02, 0.27]		[0.09, 0.43]			
1 - β		1			0.92		0.99			
R^2			**R^2_c = 0.85**					**R^2_c = 0.88**		
Minor Axis Diameter		***					***			**
p value		< 0.001					< 0.001			LL x O < 0.01
η_p^2		0.41					0.37			0.16
95% CI		[0.23, 0.54]					[0.17, 0.50]			[0.02, 0.28]
1 - β		1					0.99			0.92
R^2			**R^2_c = 0.90**					**R^2_c = 0.93**		

Table 4 (continued)

	Female					Male				
	Pain Status (PS)	Lumbar Level (LL)	Position (O)	BMI	Interaction	Pain Status (PS)	Lumbar Level (LL)	Position (O)	BMI	Interaction
Axis Ratio										*, *
p value										PS x O < 0.05 LL x O < 0.05
η_p^2										0.06 0.15
95% CI										[0.00. 0.20] [0.00, 0.28]
1 - β										0.61 0.76
R^2			**R^2_c = 0.69**						**R^2_c = 0.78**	
IV Angle		***	**	**	***		***			***
p value		< 0.001	< 0.01	< 0.01	LL x O < 0.001		< 0.001			LL x O < 0.001
η_p^2		0.71	0.09	0.39	0.19		0.67			0.19
95% CI		[0.59, 0.78]	[0.01, 0.21]	[0.06, 0.63]	[0.05, 0.31]		[0.53, 0.75]			[0.04, 0.31]
1 - β		1	0.87	0.89	0.98		1			0.96
R^2			**R^2_c = 0.77**						**R^2_c = 0.75**	
AP Ratio		***			***		***			***
p value		< 0.001			LL x O < 0.001		< 0.001			LL x O < 0.001
η_p^2		0.51			0.23		0.58			0.23
95% CI		[0.34, 0.62]			[0.08, 0.35]		[0.42, 0.69]			[0.07, 0.36]
1 - β		1			0.99		1			0.99
R^2			**R^2_c = 0.73**						**R^2_c = 0.66**	
Width		**					***			
p value		< 0.01					< 0.001			
η_p^2		0.2					0.39			
95% CI		[0.04, 0.33]					[0.20, 0.53]			
1 - β		0.95					1			
R^2			**R^2_c = 0.79**						**R^2_c = 0.92**	
NIDI		***	***		*		***	***		
p value		< 0.001	< 0.001		PS x O < 0.05		< 0.001	< 0.001		
η_p^2		0.24	0.15		0.05		0.37	0.25		
95% CI		[0.07, 0.38]	[0.04, 0.30]		[0.00, 0.17]		[0.18, 0.51]	[0.08, 0.43]		
1 - β		0.97	0.92		0.50		0.99	0.99		
R^2			**R^2_c = 0.81**						**R^2_c = 0.81**	
Degeneration			***		*		***	***		**
p value		= 0.056	< 0.001		LL x O < 0.05		< 0.001	< 0.001		LL x O < 0.01
η_p^2		0.13	0.11		0.09		0.32	0.23		0.18
95% CI		[0.00, 0.25]	[0.02, 0.24]		[0.00, 0.19]		[0.12, 0.46]	[0.09, 0.37]		[0.04, 0.31]
1 - β		0.67	0.95		0.69		0.99	0.99		0.96
R^2			**R^2_c = 0.99**						**R^2_c = 0.99**	
Cobb Angle			*							
p value			< 0.05							
η_p^2			0.23							
95% CI			[0.00, 0.47]							
1 - β			0.58							
R^2			**R^2_c = 0.92**						**R^2_c = 0.92**	

Differences in Initial Standing

After initially assuming the standing position, pain was not a significant main nor interaction factor influencing any IVD morphology or Cobb angle. In standing, there was a trending difference between female L5S1 and L2L3 Degeneration ($p = 0.053$; Tukey). As in supine, the male L5S1 level was more degenerated than all other discs by at least 15.31 ($p < 0.01$ for all comparisons; Tukey).

Table 5

Model results of comparisons in initial standing.

	Female				Male			
	Pain Status (PS)	Lumbar Level (LL)	BMI	PS x LL	Pain Status (PS)	Lumbar Level (LL)	BMI	PS x LL
IVD Volume		***				***		
p value		< 0.001				< 0.001	= 0.10	
η_p^2		0.60				0.59	0.01	
95% CI		[0.45, 0.69]				[0.40, 0.70]	[0.00, 0.23]	
1 - β		1				1	0.58	
R^2		**R^2_c = 0.79**				**R^2_c = 0.82**		
NP Volume		***				***		
p value		< 0.001				< 0.001		
η_p^2		0.56				0.50		
95% CI		[0.40, 0.66]				[0.30, 0.62]		
1 - β		1				1		
R^2		**R^2_c = 0.77**				**R^2_c = 0.68**		
NP Volume Fraction		*				***		
p value		< 0.05				< 0.001		
η_p^2		0.15				0.42		
95% CI		[0.01, 0.28]				[0.19, 0.56]		
1 - β		0.8				0.99		
R^2		**R^2_c = 0.68**				**R^2_c = 0.74**		
Disc Height		***				***		
p value	= 0.053	< 0.001	= 0.059			< 0.001	= 0.09	
η_p^2	0.19	0.60	0.20			0.59	0.18	
95% CI	[0.00, 0.49]	[0.44, 0.70]	[0.00, 0.50]			[0.41, 0.70]	[0.00, 0.49]	
1 - β	0.50	1	0.48			1	0.41	
R^2		**R^2_c = 0.60**				**R^2_c = 0.59**		
Major Axis Diameter		***				***		
p value		< 0.001				< 0.01		
η_p^2		0.37				0.3		
95% CI		[0.17, 0.50]				[0.08, 0.46]		
1 - β		0.99				0.97		
R^2		**R^2_c = 0.74**				**R^2_c = 0.67**		
Minor Axis Diameter		***				***		
p value		< 0.001				< 0.001		
η_p^2		0.45				0.39		
95% CI		[0.26, 0.57]				[0.29, 0.52]		
1 - β		1				1		
R^2		**R^2_c = 0.82**				**R^2_c = 0.84**		

Table 5 (continued)

	Female				Male			
	Pain Status (PS)	Lumbar Level (LL)	BMI	PS x LL	Pain Status (PS)	Lumbar Level (LL)	BMI	PS x LL
Axis Ratio								
p value								
η_p^2								
95% CI								
1 - β								
R^2		**R^2_c = 0.52**				**R^2_c = 0.46**		
IV Angle		***	**			***		
p value		< 0.001	< 0.01	= 0.10		< 0.001		
η_p^2		0.55	0.34	0.10		0.44		
95% CI		[0.39, 0.65]	[0.03, 0.60]	[0.00, 0.21]		[0.25, 0.57]		
1 - β		1	0.81	0.59		1		
R^2		**R^2_c = 0.57**				**R^2_c = 0.49**		
AP Ratio		***				***		
p value		< 0.001				< 0.001		
η_p^2		0.28				0.38		
95% CI		[0.10, 0.41]				[0.18, 0.51]		
1 - β		0.99				1		
R^2		**R^2_c = 0.30**				**R^2_c = 0.37**		
Width		**				***		
p value		< 0.01				< 0.001		
η_p^2		0.16				0.32		
95% CI		[0.01, 0.29]				[0.12, 0.46]		
1 - β		0.87				0.99		
R^2		**R^2_c = 0.66**				**R^2_c = 0.87**		
NIDI		*				**		
p value		< 0.05				< 0.01		
η_p^2		0.20				0.29		
95% CI		[0.02, 0.34]				[0.03, 0.46]		
1 - β		0.83				0.90		
R^2		**R^2_c = 0.37**				**R^2_c = 0.42**		
Degeneration		*				***		
p value		< 0.05				< 0.001		
η_p^2		0.13				0.34		
95% CI		[0.00, 0.25]				[0.14, 0.47]		
1 - β		0.70				0.99		
R^2		**R^2_c = 0.17**				**R^2_c = 0.29**		
Cobb Angle								
p value			= 0.053					
η_p^2			0.19					
95% CI			[0.00, 0.48]					
1 - β								
R^2		**R^2 = 0.21**				**R^2 < 0.01**		

Differences during Prolonged Standing

There was a significant effect of pain on female disc height ($p = 0.0066$) with a large effect size. Female NPD disc height was estimated at 9.86 mm and PD disc height at 9.12 mm with 95% confidence intervals of [9.48, 10.24] and [8.79, 9.45] respectively. Despite the significant interaction of standing time and pain, post hoc comparisons between NPDs and PDs showed no significant difference in WD volume at any time point. There is a trending difference in female WD volume of 2.32 cm^3 ($p = 0.06$). PDs also showed different NIDI trajectories while standing from NPDs as shown in Figure 6.

Table 6

Model results of comparisons during prolonged standing.

	Female					Male				
	Pain Status (PS)	Lumbar Level (LL)	Standing Time (ST)	BMI	Interaction	Pain Status (PS)	Lumbar Level (LL)	Standing Time (ST)	BMI	Interaction
IVD Volume		***	**		***		***			
p value	= 0.06	< 0.001	< 0.01		PS x ST < 0.001		< 0.001			PS x ST = 0.097
η_p^2	0.19	0.63	0.04		0.08		0.65			0.03
95% CI	[0.00 , 0.48]	[0.49, 0.72]	[0.00, 0.06]		[0.03, 0.12]		[0.50, 0.74]			[0.00, 0.052]
1 - β	0.49	1	0.923		1		1			0.71
R^2			**R^2_c = 0.95**					**R^2_c = 0.94**		
NP Volume		***	***		***		***			
p value		< 0.001	< 0.001		PS x ST < 0.001		< 0.001			
η_p^2		0.49	0.09		0.05		0.52			
95% CI		[0.31, 0.60]	[0.05, 0.13]		[0.01, 0.08]		[0.34, 0.63]			
1 - β		1	1		0.99		1			
R^2			**R^2_c = 0.93**					**R^2_c = 0.95**		
NP Volume Fraction		**	***				***			
p value		< 0.01	< 0.001				< 0.001			
η_p^2		0.18	0.07				0.45			
95% CI		[0.03, 0.31]	[0.01, 0.10]				[0.25, 0.58]			
1 - β		0.88	0.99				1			
R^2			**R^2_c = 0.70**					**R^2_c = 0.86**		
Disc Height	**	***		*			***			
p value	< 0.01	< 0.001	= 0.09	< 0.05			< 0.001			
η_p^2	0.31	0.59	0.02	0.23			0.65			
95% CI	[0.02, 0.58]	[0.43, 0.68]	[0.00, 0.04]	[0.00, 0.52]			[0.51, 0.74]			
1 - β	0.83	1	0.73	0.59			1			
R^2			**R^2_c = 0.90**					**R^2_c = 0.93**		
Major Axis Diameter		***	*		***		***			**
p value	= 0.06	< 0.001	< 0.05		PS x ST < 0.001		< 0.001			PS x ST < 0.01
η_p^2	0.21	0.62	0.03		0.05		0.44			0.05
95% CI	[0.00, 0.50]	[0.48, 0.71]	[0.00, 0.05]		[0.01, 0.08]		[0.24, 0.57]			[0.01, 0.09]
1 - β	0.48	1	0.85		0.98		1			0.94
R^2			**R^2_c = 0.85**					**R^2_c = 0.83**		
Minor Axis Diameter		***			*		***			*
p value		< 0.001			PS x ST < 0.05		< 0.001			PS x LL < 0.05
η_p^2		0.52			0.03		0.42			0.15
95% CI		[0.35, 0.63]			[0.00, 0.05]		[0.23, 0.55]			[0.00, 0.28]
1 - β		1			0.84		1			0.94
R^2			**R^2_c = 0.94**					**R^2_c = 0.95**		

Table 6 (continued)

	Female					Male				
	Pain Status (PS)	Lumbar Level (LL)	Standing Time (ST)	BMI	Interaction	Pain Status (PS)	Lumbar Level (LL)	Standing Time (ST)	BMI	Interaction
Axis Ratio			*							
p value			< 0.05		PS x ST = 0.067		= 0.10			PS x ST = 0.07
η_p^2			0.02		0.03		0.12			0.03
95% CI			[0.00, 0.04]		[0.00, 0.05]		[0.00, 0.25]			[0.00, 0.06]
1 - β			0.81		0.76		0.58			0.75
R^2			**R^2_c = 0.74**					**R^2_c = 0.71**		
IV Angle		***		**			***			*
p value		<0.001		< 0.01	PS x ST = 0.09		< 0.001	= 0.09		PS x ST < 0.05
η_p^2		0.65		0.38	0.02		0.61	0.02		0.03
95% CI		[0.51, 0.73]		[0.06, 0.63]	[0.00, 0.03]		[0.45, 0.71]	[0.00, 0.04]		[0.00, 0.02]
1 - β		1		0.88	0.72		1	0.719		0.85
R^2			**R^2_c = 0.79**					**R^2_c = 0.75**		
AP Ratio		***					***			
p value		< 0.001					< 0.001			
η_p^2		0.52					0.49			
95% CI		[0.35, 063]					[0.31, 0.61]			
1 - β		1					1			
R^2			**R^2_c = 0.65**					**R^2_c = 0.58**		
Width		***					***			
p value		< 0.001					< 0.001			PS x LL = 0.07 PS x ST = 0.09
η_p^2		0.35					0.39			0.12 0.02
95% CI		[0.17, 0.48]					[0.19, 0.52]			[0.00, 0.27] [0.00, 0.04]
1 - β		1					0.99			0.63 0.73
R^2			**R^2_c = 0.87**					**R^2_c = 0.93**		
NIDI		**	***		**		***			**
p value		< 0.01	< 0.001		PS x ST < 0.001		< 0.001	= 0.06	=0.07	PS x ST < 0.01
η_p^2		0.22	0.17		0.04		0.31	0.04	0.22	0.06
95% CI		[0.04, 0.35]	[0.10, 0.23]		[0.00, 0.07]		[0.10, 0.45]	[0.00, 0.06]	[0.00, 0.53]	[0.01, 0.10]
1 - β		0.91	1		0.91		0.99	0.77	0.45	0.96
R^2			**R^2_c = 0.87**					**R^2_c = 0.84**		
Cobb Angle				*						
p value				< 0.05						
η_p^2				0.26						
95% CI				[0.00, 0.54]						
1 - β				0.67						
R^2			**R^2_c = 0.91**					**R^2_c = 0.91**		

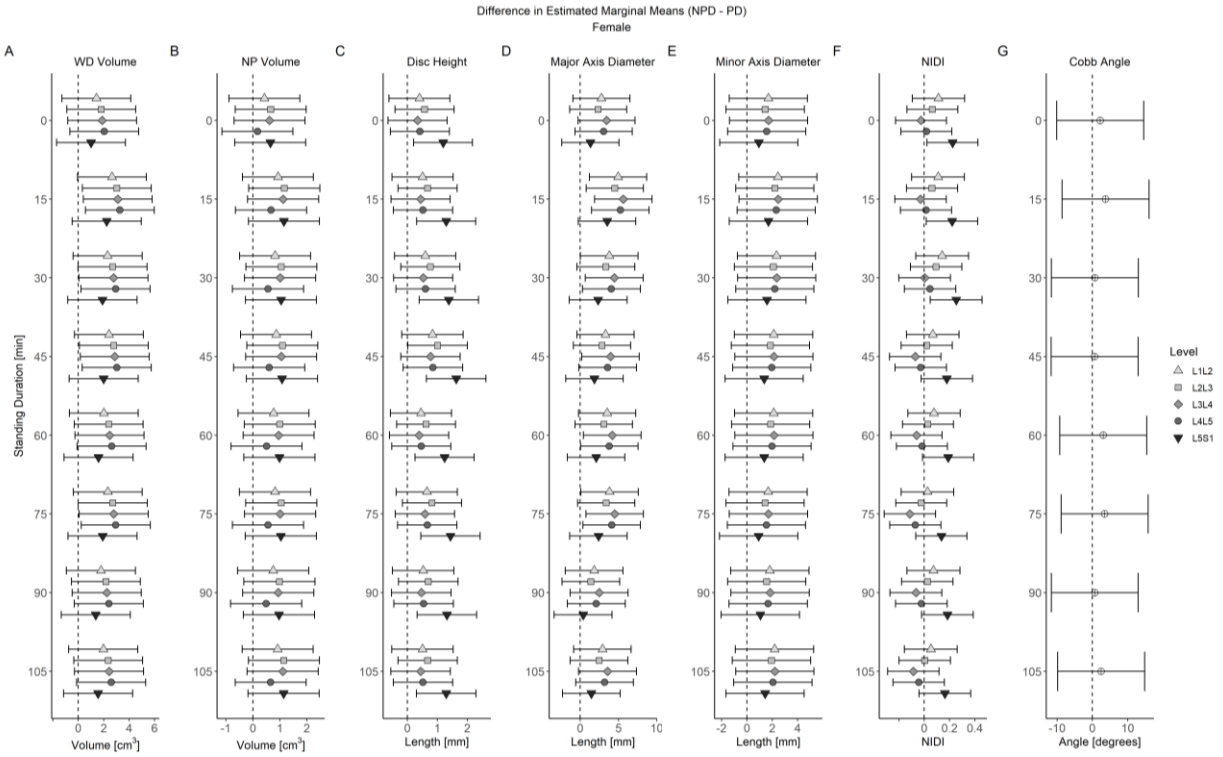

Figure 4. Comparisons of female NPDs and PDs for Cobb angle and measurements in which the main effect of pain or an interaction with pain was identified as significant. Error bars denote 95% confidence intervals on the mean difference. These variables included: A) Whole disc volume; B) NP volume; C) Disc height; D) Major axis diameter; E) Minor axis diameter; F) NIDI; G) Cobb angle. *Note: As this is an exploratory study, these comparisons between NPDs and PDs within each level and time point are pre-planned comparisons with no corrections made for multiple comparisons*.

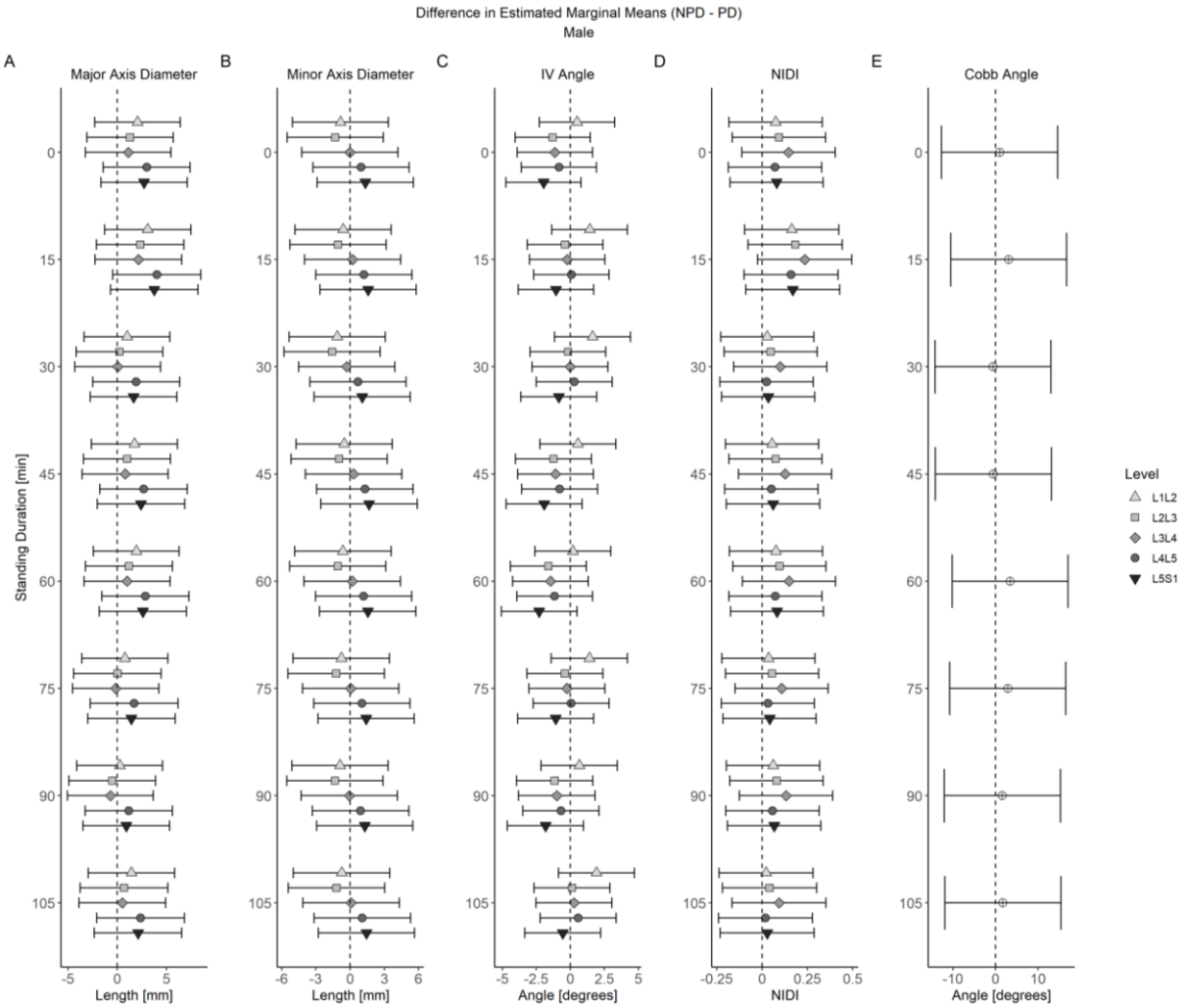

Figure 5. Comparisons of male NPDs and PDs for Cobb angle and measurements in which the main effect of pain or an interaction with pain was identified as significant. Error bars denote 95% confidence intervals on the mean difference. These variables included: A) Major axis diameter; B) Minor axis diameter; C) IV angle; D) NIDI; and E) Cobb angle. *Note: As this is an exploratory study, these comparisons between NPDs and PDs within each level and time point are pre-planned comparisons with no corrections made for multiple comparisons.*

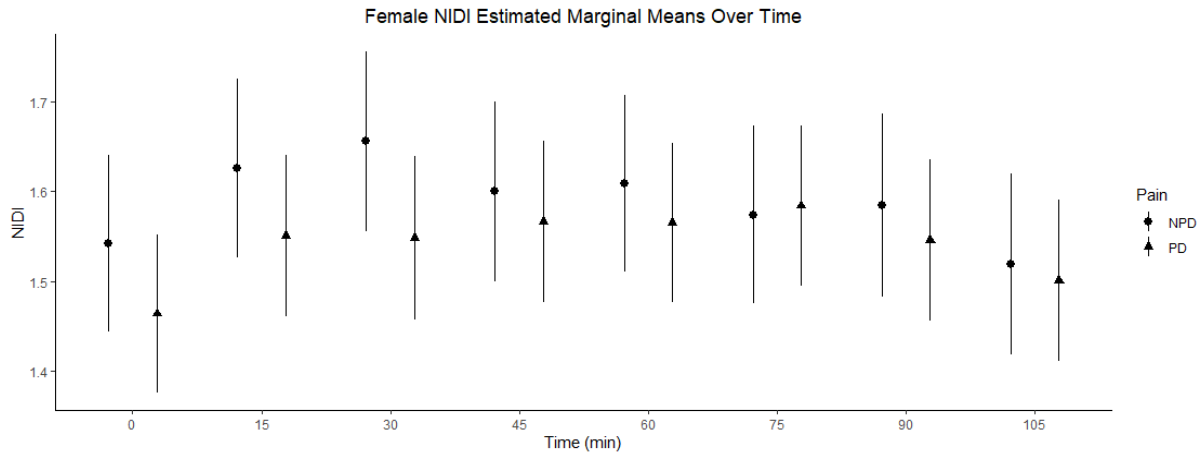

Figure 6. Female PDs show different NIDI trajectories from NPDs. In NPDs, NIDI increased at first, with 0 minutes being different from 15 and 30 minutes and later decreased with NIDI at 30, 45, and 60 minutes being greater than at 105 minutes. NIDI was also elevated at 30 minutes relative to 75 and 105 minutes. In PDs, there was a less dynamic increase, with NIDI at 0 being different from 15, 30, 45, 60, 75, and 90 minutes and NIDI at 75 minutes being greater than at 105 minutes ($p < 0.05$ for all comparisons, Šidák).

VAS Mixed Model

A multivariate mixed model was fitted with the log-transformed non-zero VAS scores as the response variable. To combat loss of observations due to missingness of any predictor measurement, missing measurements were imputed in this analysis. The best predictors for males and females were determined by backward selection on the set of features shown in Figures 4 and 5 respectively. Despite the absence of a significant effect of pain on Cobb angle in males or females, Cobb angle was included in the set for its theoretical association with LBP. The models were also run with best predictors from the set of clinically available features including Cobb angle, width, IV angle, and AP ratio.

The selected best predictors for females were L5S1 WD volume, L2L3 and L5S1 NIDI, and Cobb angle. The female model identified only L2L3 NIDI as a significant factor that is negatively related to pain ($p = 0.029$; $R_c^2 = 0.38$). The selected best predictors for males were L2L3 NIDI and L1L2 IV angle. In this model, L2L3 NIDI was also identified as a significant factor having a negative relationship with pain ($p = 0.026$; $R_c^2 = 0.21$). The clinical best predictors for females were L3L4 and L5S1 AP ratios, and L4L5 width. All factors were significantly related to the pain outcome. L5S1 and L3L4 AP ratios were negatively related to pain outcome ($p = 0.002$, $p = 0.006$) while L4L5 width was positively related to pain outcome ($p < 0.001$; $R_c^2 = 0.35$). The clinical best predictors for males were L1L2 and L2L3 AP ratio and L5S1 width. The model identified L1L2 AP ratio and L5S1 width as significant factors both having negative relationships with pain ($p = 0.031$, $p = 0.003$; $R_c^2 = 0.44$).

Pain AUC and Max VAS Correlations

The subject that completed only two standing time points was excluded from correlation analyses involving pain AUC and max VAS because their standing duration was too dissimilar from other PDs. Correlations with pain AUC were made with measurements per disc and Cobb angle averaged across standing time points. The correlations with max VAS were performed on the same measurements except only those measured at the time of maximum pain. Pearson correlation coefficients for all relationships and those with moderate relationships (abs(r) > 0.50) that could reasonably influence pain were tested for significance. After adjusting for multiple tests of significance, the remaining significant correlations are reported in Table 7.

Table 7

Significant correlations with Pain AUC and Max VAS. The reported p values are Šidák adjusted to account for multiple correlations.

	Female (r, *p value*)		**Male** (r, *p value*)	
	Max VAS	**Pain AUC**	**Max VAS**	**Pain AUC**
L1L2 Width			(-0.84, 0.038)	
L2L3 NIDI				(-0.91, 0.010)
L4L5 AP	(0.79, 0.008)			
L3L4 IV Angle	(0.59, 0.018)			
L4L5 IV Angle	(0.78, 0.012)	(0.80, 0.010)		

Chapter 4: Discussion

This study explored the morphological differences of the lumbar IVDs between PDs and NPDs in the supine and standing positions as well as the correlative relationships between IVD morphology and pain outcomes. We recruited 40 participants and imaged them using T2 MRI over 8 time points of standing. Half the participants developed LBP symptoms during the standing time course, consistent with the prevalence reported by other studies [23,24,26]. We developed and validated a set of repeatable and reliable IVD morphometric measurements from volumetric MRI in the supine and standing positions.

Our previous work showed that standing position alters the lumbar spine morphology from the supine position [34]. Unsurprisingly, the current study shows that measurements made in the supine position are insufficient to differentiate PDs from NPDs. We also identified potential imaging biomarkers that distinguish PDs from NPDs, such as a reduction in NIDI of female PDs upon standing. These differences confirm the utility of imaging in functionally relevant positions. We found that inclusion of temporally longitudinal MRI images improves the prediction of pain status and magnitude.

The pain status of an individual was not associated with any specific morphological characteristics at any segmental level in the supine position. This finding suggests that if pain is discogenic, morphological changes to the IVDs do not present until they take on greater loading conditions. In fact, we discovered that the signal intensity of the L5S1 NP exhibits a small but significant change following the transition from supine to standing in females PDs while female NPDs show no such change. The loss of signal intensity on MRI is associated with loss of water content and is consistent with a load-induced adaptation as the axial compressive loads from

standing forces matrix water to gradually exude from the NP. This susceptibility to loss of hydration during standing could progress into pathological degeneration.

Female PDs exhibited the most notable differences in IVD morphology. Female PDs showed reduced disc heights throughout the standing task. It is interesting to note that there was no significant difference in supine or at the initial standing time point, and that the difference only appeared after consulting with height across time in standing (although there was a trending difference in female disc height in the standing position, $p = 0.053$). A recent radiographic study demonstrated that among individuals with early to middle stage disc degeneration, those with discogenic LBP show greater disc height discrepancy in between supine and standing positions than those without [43]. Pairwise comparisons between PDs and NPDs at all disc levels and time points indicated that the difference could be primarily driven by the L5S1 disc level. The L5S1 IVD was also the most significantly degenerated of the male discs. The IVD at this level has the most unique geometry and loading conditions relative to the other lumbar IVDs, and we found that it alone experiences changes to IV angle and AP ratio both of which indicate that the load incurred upon standing causes significant deformations at this level. We also showed that the lower levels, L5S1 and L4L5, have the lowest NIDIs. In females, NIDI changed over time differently between PDs and NPDs, with both showing a rise and fall in NIDI throughout standing, but with PDs showing a less dynamic change across time. Changes to the signal intensity of the discs are not surprising as signal intensity has been shown to continuously increase over a period of around 6 hours in simulated loading conditions in a supine MRI [44]. Our findings could mean that changes in water content of the NP are associated with standing-induced LBP. The findings on females could indicate that involvement of the IVD in standing-induced LBP is sex specific.

L2L3 NIDI was related to the pain of PDs in both males and females. Both relationships were negative with pain indicating that lower NIDIs were associated with greater pain. The same relationship reappeared as a significant correlation with male L2L3 NIDI being negatively correlated with pain AUC. Such a trend is reasonable since one aspect of painful, degenerated discs is low signal intensity from the NP. Among the clinically available predictors, increases in female VAS were associated with decreases in AP ratio at two segmental levels and increases in L4L5 width. This would suggest that less wedging of the L5S1 and L3L4 and greater anteroposterior bulging of the L4L5 disc is associated with greater pain for females. In males, reductions in L1L2 AP ratios and L5S1 widths were associated with greater pain.

Unlike others, we did not find any differences in lordosis between PDs and NPDs in the initial standing position [26]. We also found no lordotic differences throughout the prolonged standing task. Degenerative grading, which was performed both in the supine and initial standing positions, was not predictive in this population highlighting the need for other quantitative metrics in assessing the overall properties IVDs that appear healthy. Our findings for female PDs share some similarities with the criteria that were used to grade degeneration, namely disc height and the signal intensity of the NP relative to the whole disc; As no difference in degeneration was found among females, there may be a need for a more quantitative system of grading early degeneration. Future investigations of standing-induced LBP may consider computing NIDI from either single slice MRI or volumetric images. This study also demonstrates the role of standing in bringing about these differences. Future work on clinical LBP populations could benefit from pMRI imaging on the lumbar spine in functionally relevant positions.

This study utilized a method of measuring disc height directly from segmentations. Disc height is frequently measured as the length of one or more lines connecting the inferior and

superior surfaces of the IVD in a sagittal view [45], but there is no standard approach. Others have measured disc height directly from segmentation on high resolution MRI scans on ex-vivo samples by dividing the whole volume by the axial area [46]. Some groups have analyzed the geometric deformations of the lumbar IVDs in standing by defining local disc height according to the distance between nearest points within contour-defined meshes of the upper and lower disc surface along the z-axis of a reference coordinate system centered on and oriented with respect to the lower endplate [47]. Moreover, others have used segmentations on MRI to map height across the disc by applying a method of Laplacian thickness [48]. One limitation of our method is that it assumes healthy discs to be roughly ellipsoidal. PCA results in vectors that are orthogonal to one another which is well suited to describing discs that exhibit symmetry about a set of orthogonal planes. IVDs deviate from this assumption when they present wedge-like morphology which is especially likely at the L5S1 disc level. Nevertheless, this automated segmentation-based process for measuring disc height yielded the highest reliability among other morphometry performed by the researcher.

There were some noteworthy limitations to our study. While the short sequencing time likely reduced the presence of motion artifacts among the images we obtained, some measurements were not possible due to blurring. We encountered unexpected loss of observations due to misalignment of the subject and the scanner's field of view. These losses reduced our ability to detect differences in whole disc volume, major axis diameter, and axis ratio. Although we obtained acceptable images from standing individuals, the data quality would likely be improved with a higher resolution scanner. We were also limited by the number of male PDs. With only 8 male PDs, our power to detect differences associated with pain was reduced. The additional missing observations from the subject that was only imaged for two time points

compounded this issue. In future studies looking to perform volumetric morphometry from MRI on standing subjects, more precautions should be taken to ensure that subjects do not exit the field of view or so that the field of view is more permissive of small positional adjustments.

Chapter 5: Conclusions

We demonstrated reliable measurements of IVD morphology via volumetric positional MRI images taken in the supine and standing positions. Females exhibited the only morphological differences between PDs and NPDs. The signal intensity of the NP relative to the surrounding tissue became an important parameter in distinguishing between groups and showed some relationship with pain outcomes in both sexes. We discovered that female PDs have reduced disc heights relative to NPDs, and that imaging in the standing position was necessary for this difference to manifest, further promoting the idea that functionally relevant imaging could be important when addressing LBP.

References

1. Andersson GB. Epidemiological features of chronic low-back pain. *The Lancet*;354. Epub ahead of print August 1999. DOI: 10.1016/S0140-6736(99)01312-4.

2. Hoy D, Brooks P, Blyth F, et al. The Epidemiology of low back pain. *Best Practice and Research: Clinical Rheumatology*;24. Epub ahead of print 2010. DOI: 10.1016/j.berh.2010.10.002.

3. Manchikanti L, Singh V, Falco FJE, et al. Epidemiology of low back pain in Adults. *Neuromodulation*;17. Epub ahead of print 2014. DOI: 10.1111/ner.12018.

4. Lawrence RC, Helmick CG, Arnett FC, et al. Estimates of the prevalence of arthritis and selected musculoskeletal disorders in the United States. *Arthritis and Rheumatism*;41. Epub ahead of print 1998. DOI: 10.1002/1529-0131(199805)41:5<778::AID-ART4>3.0.CO;2-V.

5. Katz JN. Lumbar Disc Disorders and Low-Back Pain: Socioeconomic Factors and Consequences. *Journal of Bone and Joint Surgery*;88. Epub ahead of print April 2006. DOI: 10.2106/JBJS.E.01273.

6. Hoy D, March L, Brooks P, et al. The global burden of low back pain: Estimates from the Global Burden of Disease 2010 study. *Annals of the Rheumatic Diseases*;73. Epub ahead of print 2014. DOI: 10.1136/annrheumdis-2013-204428.

7. Maher C, Underwood M, Buchbinder R. Non-specific low back pain. *The Lancet*;389. Epub ahead of print 2017. DOI: 10.1016/S0140-6736(16)30970-9.

8. Wu A, March L, Zheng X, et al. Global low back pain prevalence and years lived with disability from 1990 to 2017: estimates from the Global Burden of Disease Study 2017. *Annals of Translational Medicine*;8. Epub ahead of print 2020. DOI: 10.21037/atm.2020.02.175.

9. Hartvigsen J, Hancock MJ, Kongsted A, et al. What low back pain is and why we need to pay attention. *The Lancet*;391. Epub ahead of print 2018. DOI: 10.1016/S0140-6736(18)30480-X.

10. Chenot JF, Becker A, Leonhardt C, et al. Sex differences in presentation, course, and management of low back pain in primary care. *Clinical Journal of Pain*;24. Epub ahead of print 2008. DOI: 10.1097/AJP.0b013e31816ed948.

11. Chou R, Qaseem A, Snow V, et al. Diagnosis and treatment of low back pain: A joint clinical practice guideline from the American College of Physicians and the American Pain Society. *Annals of Internal Medicine*;147. Epub ahead of print 2007. DOI: 10.7326/0003-4819-147-7-200710020-00006.

12. Francois SJ, Lanier VM, Marich A v., et al. A Cross-Sectional Study Assessing Treatment Preference of People With Chronic Low Back Pain. *Archives of Physical Medicine and Rehabilitation*;99. Epub ahead of print 2018. DOI: 10.1016/j.apmr.2018.04.027.

13. Krismer M, van Tulder M. Low back pain (non-specific). *Best Practice & Research Clinical Rheumatology*;21. Epub ahead of print February 2007. DOI: 10.1016/j.berh.2006.08.004.

14. Verrills P, Nowesenitz G, Barnard A. Prevalence and Characteristics of Discogenic Pain in Tertiary Practice: 223 Consecutive Cases Utilizing Lumbar Discography. *Pain Medicine (United States)*;16. Epub ahead of print 2015. DOI: 10.1111/pme.12809.

15. Brinjikji W, Diehn FE, Jarvik JG, et al. MRI findings of disc degeneration are more prevalent in adults with low back pain than in asymptomatic controls: A systematic review and meta-analysis. *American Journal of Neuroradiology*;36. Epub ahead of print 2015. DOI: 10.3174/ajnr.A4498.

16. van Dillen LR, Sahrmann SA, Norton BJ, et al. Movement system impairment-based categories for low back pain: Stage 1 validation. *Journal of Orthopaedic and Sports Physical Therapy*;33. Epub ahead of print 2003. DOI: 10.2519/jospt.2003.33.3.126.

17. Fritz JM, Cleland JA, Childs JD. Subgrouping patients with low back pain: Evolution of a classification approach to physical therapy. *Journal of Orthopaedic and Sports Physical Therapy*;37. Epub ahead of print 2007. DOI: 10.2519/jospt.2007.2498.

18. Nelson-Wong E, Callaghan JP. Transient Low Back Pain Development During Standing Predicts Future Clinical Low Back Pain in Previously Asymptomatic Individuals. *Spine*;39. Epub ahead of print March 2014. DOI: 10.1097/BRS.0000000000000191.

19. Macfarlane GJ, Thomas E, Papageorgiou AC, et al. Employment and physical work activities as predictors of future low back pain. *Spine*;22. Epub ahead of print 1997. DOI: 10.1097/00007632-199705150-00015.

20. Xu Y, Bach E, Ørhede E. Work environment and low back pain: The influence of occupational activities. *Occupational and Environmental Medicine*;54. Epub ahead of print 1997. DOI: 10.1136/oem.54.10.741.

21. Andersen JH, Haahr JP, Frost P. Risk factors for more severe regional musculoskeletal symptoms: A two-year prospective study of a general working population. *Arthritis & Rheumatism*;56. Epub ahead of print April 2007. DOI: 10.1002/art.22513.

22. Gregory DE, Callaghan JP. Prolonged standing as a precursor for the development of low back discomfort: An investigation of possible mechanisms. *Gait & Posture*;28. Epub ahead of print July 2008. DOI: 10.1016/j.gaitpost.2007.10.005.

23. Nelson-Wong E, Gregory DE, Winter DA, et al. Gluteus medius muscle activation patterns as a predictor of low back pain during standing. *Clinical Biomechanics*;23. Epub ahead of print 2008. DOI: 10.1016/j.clinbiomech.2008.01.002.

24. Sorensen CJ, Johnson MB, Norton BJ, et al. Asymmetry of lumbopelvic movement patterns during active hip abduction is a risk factor for low back pain development during standing. *Human Movement Science*;50. Epub ahead of print 2016. DOI: 10.1016/j.humov.2016.10.003.

25. Hwang CT, van Dillen LR, Haroutounian S. Do Changes in Sensory Processing Precede Low Back Pain Development in Healthy Individuals? *Clinical Journal of Pain*;34. Epub ahead of print 2018. DOI: 10.1097/AJP.0000000000000563.

26. Sorensen CJ, Norton BJ, Callaghan JP, et al. Is lumbar lordosis related to low back pain development during prolonged standing? *Manual Therapy*;20. Epub ahead of print August 2015. DOI: 10.1016/j.math.2015.01.001.

27. Papageorgiou AC, Croft PR, Thomas E, et al. Influence of previous pain experience on the episode incidence of low back pain: results from the South Manchester Back Pain Study. *Pain*;66. Epub ahead of print August 1996. DOI: 10.1016/0304-3959(96)03022-9.

28. Sorensen CJ, Johnson MB, Callaghan JP, et al. Validity of a Paradigm for Low Back Pain Symptom Development During Prolonged Standing. *The Clinical Journal of Pain*;31. Epub ahead of print July 2015. DOI: 10.1097/AJP.0000000000000148.

29. Rodríguez-Soto AE, Jaworski R, Jensen A, et al. Effect of load carriage on lumbar spine kinematics. *Spine*;38. Epub ahead of print 2013. DOI: 10.1097/BRS.0b013e3182913e9f.

30. Ludescher B, Effelsberg J, Martirosian P, et al. T2- and diffusion-maps reveal diurnal changes of intervertebral disc composition: An in vivo MRI study at 1.5 Tesla. *Journal of Magnetic Resonance Imaging*;28. Epub ahead of print July 2008. DOI: 10.1002/jmri.21390.

31. Fedorov A, Beichel R, Kalpathy-Cramer J, et al. 3D Slicer as an image computing platform for the Quantitative Imaging Network. *Magnetic Resonance Imaging*;30. Epub ahead of print November 2012. DOI: 10.1016/j.mri.2012.05.001.

32. Gonzalo Domínguez M, Hernández C, Ruisoto P, et al. Morphological and Volumetric Assessment of Cerebral Ventricular System with 3D Slicer Software. *Journal of Medical Systems*;40. Epub ahead of print June 5, 2016. DOI: 10.1007/s10916-016-0510-9.

33. Guerroumi N, Playout C, Laporte C, et al. Automatic Segmentation of the Scoliotic Spine from Mr Images. In: *2019 IEEE 16th International Symposium on Biomedical Imaging (ISBI 2019)*. IEEE; 2019. Epub ahead of print April 2019. DOI: 10.1109/ISBI.2019.8759413.

34. Weber CI, Hwang CT, van Dillen LR, et al. Effects of standing on lumbar spine alignment and intervertebral disc geometry in young, healthy individuals determined by positional magnetic resonance imaging. *Clinical Biomechanics*;65. Epub ahead of print 2019. DOI: 10.1016/j.clinbiomech.2019.04.010.

35. Pfirrmann CWA, Metzdorf A, Zanetti M, et al. Magnetic Resonance Classification of Lumbar Intervertebral Disc Degeneration. *Spine*;26. Epub ahead of print September 2001. DOI: 10.1097/00007632-200109010-00011.

36. Niemeläinen R, Videman T, Dhillon SS, et al. Quantitative measurement of intervertebral disc signal using MRI. *Clinical Radiology*;63. Epub ahead of print March 2008. DOI: 10.1016/j.crad.2007.08.012.

37. Michopoulou SK, Costaridou L, Panagiotopoulos E, et al. Atlas-Based Segmentation of Degenerated Lumbar Intervertebral Discs From MR Images of the Spine. *IEEE Transactions on Biomedical Engineering*;56. Epub ahead of print September 2009. DOI: 10.1109/TBME.2009.2019765.

38. Tang R, Gungor C, Sesek RF, et al. Morphometry of the lower lumbar intervertebral discs and endplates: comparative analyses of new MRI data with previous findings. *European Spine Journal*;25. Epub ahead of print 2016. DOI: 10.1007/s00586-016-4405-8.

39. Efendioğlu M, Akar E. Morphometric analysis of cervical intervertebral disc space to reduce neural complications during anterior approaches to the cervical spine. *Journal of Orthopaedic Science*;26. Epub ahead of print 2021. DOI: 10.1016/j.jos.2020.03.019.

40. Akaike H. Information Theory and an Extension of the Maximum Likelihood Principle. 1998. Epub ahead of print 1998. DOI: 10.1007/978-1-4612-1694-0_15.

41. Schwarz G. Estimating the Dimension of a Model. *The Annals of Statistics*;6. Epub ahead of print 2007. DOI: 10.1214/aos/1176344136.

42. Nakagawa S, Schielzeth H. A general and simple method for obtaining R2 from generalized linear mixed-effects models. *Methods in Ecology and Evolution*;4. Epub ahead of print 2013. DOI: 10.1111/j.2041-210x.2012.00261.x.

43. Son S, Lee SG, Kim WK, et al. Disc height discrepancy between supine and standing positions as a screening metric for discogenic back pain in patients with disc degeneration. *Spine Journal*;21. Epub ahead of print 2021. DOI: 10.1016/j.spinee.2020.07.006.

44. Arun R, Freeman BJC, Scammell BE, et al. 2009 ISSLS prize winner: What influence does sustained mechanical load have on diffusion in the human intervertebral disc?: An in vivo study using serial postcontrast magnetic resonance imaging. *Spine*;34. Epub ahead of print 2009. DOI: 10.1097/BRS.0b013e3181b4df92.

45. Roberts N, Gratin C, Whitehouse GH. MRI analysis of lumbar intervertebral disc height in young and older populations. *Journal of Magnetic Resonance Imaging*;7. Epub ahead of print September 1997. DOI: 10.1002/jmri.1880070517.

46. Peloquin JM, Yoder JH, Jacobs NT, et al. Human L3L4 intervertebral disc mean 3D shape, modes of variation, and their relationship to degeneration. *Journal of Biomechanics*;47. Epub ahead of print July 2014. DOI: 10.1016/j.jbiomech.2014.04.014.

47. Wang S, Xia Q, Passias P, et al. Measurement of geometric deformation of lumbar intervertebral discs under in-vivo weightbearing condition. *Journal of Biomechanics*;42. Epub ahead of print 2009. DOI: 10.1016/j.jbiomech.2009.01.004.

48. Neubert A, Fripp J, Engstrom C, et al. Validity and reliability of computerized measurement of lumbar intervertebral disc height and volume from magnetic resonance images. *Spine Journal*;14. Epub ahead of print 2014. DOI: 10.1016/j.spinee.2014.05.023.

49. Pierpaoli C, Sarlls J, Nevo U. Polyvinylpyrrolidone (PVP) water solutions as isotropic phantoms for diffusion MRI studies. *Proc Intl Soc Mag …*;17.

Appendix: Supplemental Materials

MRI phantom signal intensity validation: It was demonstrated that T2 weighted signal intensity decreases with decreasing water content. A spherical phantom (High Performance Devices, Inc) housing 13 vials containing polyvinylpyrrolidone (PVP) solutions ranging from 0 to 50 %w/w in water was imaged at room temperature in the Open Upright scanner (resolution 1.2 mm x 1.2 mm x 6.55 mm)[49]. A modest decrease in water content results in an appreciable loss of signal intensity. These results support the implication that an increased NIDI reflects an increase in the NP water content relative to the whole disc.

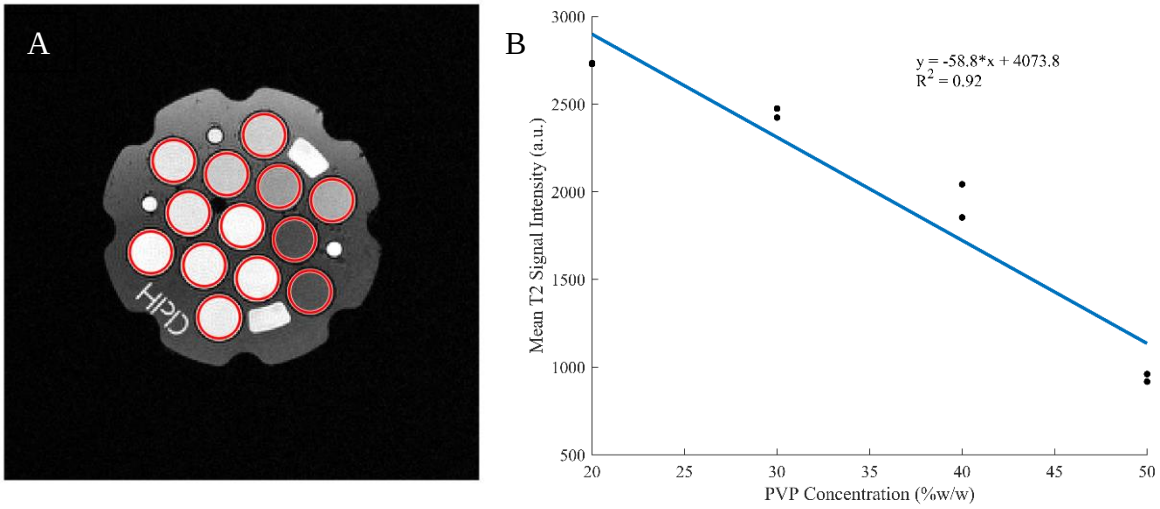

Supp Figure 1. HPD Phantom MRI signal intensity validation: A) T2 weighted image of the mid-transverse slice of the HPD phantom. ROIs for each vial were automatically detected in MATLAB and are indicated here by red circles. B) Plot of the average signal intensity within the ROIs vs PVP concentration demonstrating loss of signal intensity with decreasing water content. Note. The lowest PVP concentrations are excluded because signal intensities and water content here exceed the range relevant to this study.

Voxel size discrepancy: Nearly half of all subjects were imaged with a higher sagittal resolution (0.76mm x 0.76mm x 3.0 mm). To confirm that geometric measurements made on both resolutions yielded comparable results, five participants with high resolution scans were randomly selected and three of their IVDs were re-measured after downsampling the images to the lower resolution. Intra-rater ICCs were computed as previously described for WD volume, NP volume, disc height, major axis diameter and minor axis diameter resulting in ICCs of 0.94, 0.92, 0.87, 0.86, 0.95 respectively.

Multicollinearity of variables: Recorded measurements were determined to be too highly correlated and thus susceptible to multicollinearity with other measurements if the Pearson correlation coefficient between the two measurements exceeded 0.75. In such cases, the measurement most theoretically associated with pain or that was least susceptible to being influenced by image quality was included in the model.

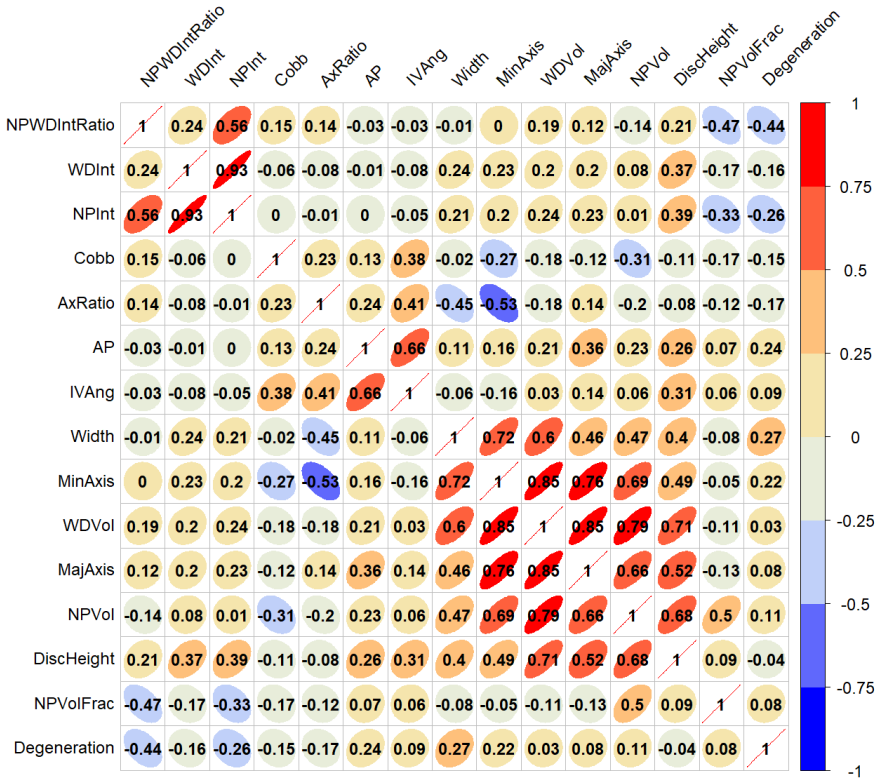

Supp Figure 2. Table of Pearson correlation coefficients of all measured parameters. Strength of correlations are color mapped between -1 and 1. In addition, positive correlations are denoted by ellipses with positive sloping major axes, and negative slopes are denoted by ellipses with negative sloping major axes.